

A Simplified Approach for Dynamic Contact Angle Measurements

Yunqian Zou, Naomi Ross, Wasim Nawaj, and Eric Borguet*



Cite This: *J. Chem. Educ.* 2024, 101, 3883–3890



Read Online

ACCESS |

Metrics & More

Article Recommendations

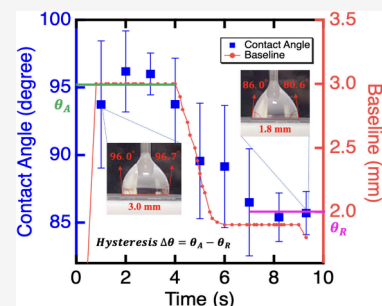
Supporting Information

ABSTRACT: Contact angle measurement is a valuable tool for analyzing surface properties, including surface structure, cleanliness, and solid–liquid interactions. Typically, this measurement is performed at the static state, capturing the interactions at the solid–liquid interface when the gas, liquid, and solid phases reach equilibrium. In this study, we developed a user-friendly setup for accurately measuring dynamic contact angles using the needle-in-drop method. Our setup consists of a syringe for controlled liquid dispensing and withdrawal on a solid surface, a sample stage with a scale bar for baseline measurements (the diameter of the droplet), a lens to magnify the image of the droplet on the solid surface, and a smartphone camera for recording the dynamic expansion and retraction of the liquid droplet. In addition to obtaining the static sessile-drop contact angle information, our modified setup allows for the acquisition of other relevant parameters, including contact angle hysteresis and the contact-line pinning force. By training students to assemble a cost-effective contact angle measurement setup using laboratory components and guiding them in the utilization of this setup for conducting static and dynamic contact angle measurements, students gain practical experience to determine the surface wettability and interfacial energy from static contact angle measurements and to characterize the interfacial hysteresis and liquid mobility from dynamic contact angle measurements. We anticipate that this approach will benefit students in a wide range of disciplines, including materials science, chemical engineering, and physical chemistry, where understanding surface properties is essential.

KEYWORDS: (Audience): Upper-Division Undergraduate, Lab Researcher,

(Domain): Analytical Chemistry, Surface Science, Laboratory Classes, (Pedagogy): User-friendly Setup, Easy-to-Assemble, Low-cost,

(Topic): Dynamic Contact Angle Measurement Setup



Contact angle measurement is a method which characterizes the solid–liquid interface interaction through visualizing the shape of a liquid droplet on the surface of a solid, determined by the surface tension between the solid and liquid.^{1,2} The interaction between the liquid and the solid surface is affected by various factors such as surface charge, surface ionizability, surface roughness, surface functional group, surface crystal structure, liquid ionizability, pH of liquid, pressure, temperature, and humidity of the surrounding air.^{3–6} The surface tension can be measured quantitatively by the tangent of the contact angle (θ) formed between the liquid and the solid surface. Qualitatively, using water droplets, surfaces are characterized as super hydrophilic ($\theta \leq 5^\circ$), hydrophilic ($5^\circ < \theta < 90^\circ$), hydrophobic ($90^\circ \leq \theta$), or superhydrophobic ($150^\circ \leq \theta$).⁷ The equilibrium between the surface tension of the air–liquid (γ_L), solid–liquid (γ_{SL}), and air–solid (γ_S) interfaces can be written as the Young-Dupre equation, see eq 1, is the measured contact angle:⁸

$$\cos \theta = \frac{\gamma_S - \gamma_{SL}}{\gamma_L} \quad (1)$$

A small contact angle suggests a smoother surface with attractive solid–liquid interactions. Conversely, a large contact angle indicates a rougher surface with weaker solid–liquid interactions. Surface roughness⁹ and contamination^{10,11}

significantly influence measured contact angles. Rough surfaces have larger surface areas than the smooth ones, but not all surface sites are accessible by liquid, resulting in weaker liquid–surface interactions and larger contact angles.¹² Contamination increases surface roughness and forms a barrier between the surface and the liquid, changing the contact angle.¹³

The hydrophilicity of the surface can be determined from both static and dynamic contact angle measurements. The static contact angle measurement (Figure 1A) is used to determine the wettability of the surfaces. This is done by adding a drop of liquid onto the surface and measuring the degree of spreading when the surface tension between the solid, liquid, and gas molecules establishes an equilibrium. The typical method for static contact angle measurement is the sessile-drop, in which a droplet of liquid is placed onto the sample surface and students record the contact angle when the droplet stops spreading and reaches a state of rest.^{8,14} The

Received: February 7, 2024

Revised: June 17, 2024

Accepted: June 24, 2024

Published: August 14, 2024



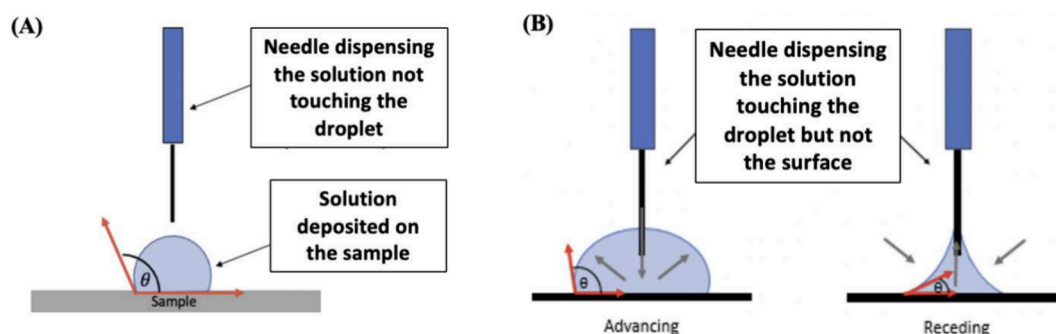


Figure 1. Static and dynamic contact angle measurements. (A) Diagram of the static sessile-drop process. A needle and syringe are used to dispense liquid onto the sample surface without the needle penetrating the drop. A contact angle measurement is taken from an image of the drop on the surface. (B) Diagram of the dynamic needle-in-drop measurement for advancing and receding contact angle measurements. The advancing contact angle is measured as the syringe dispenses the liquid onto the surface. The receding contact angle is measured as the syringe withdraws the liquid from the surface. The shape of the drop changes as the volume dispensed on the surface is adjusted.

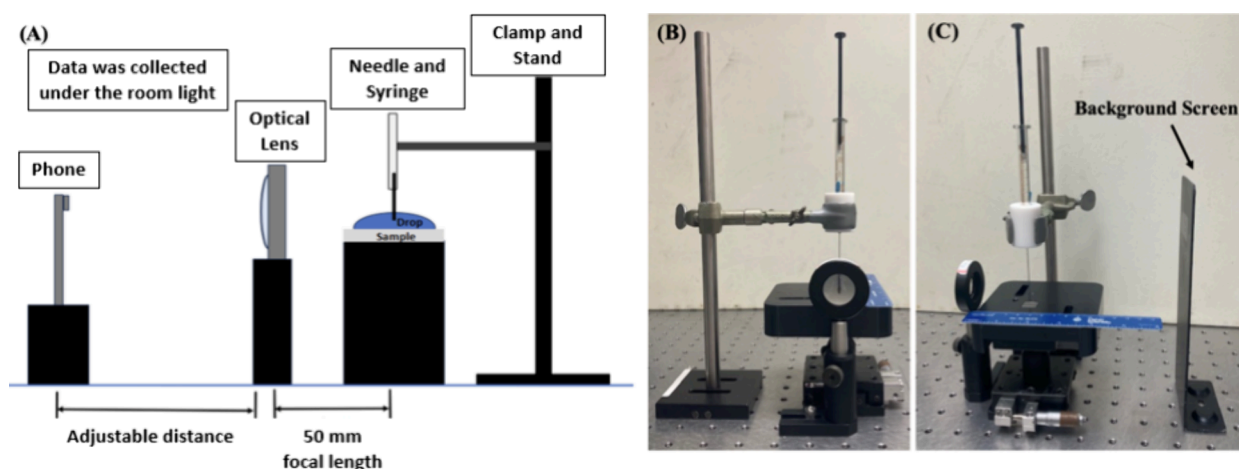


Figure 2. The diagrammatic layout of contact angle measurement and the practical arrangement achieved. (A) A schematic view of the dynamic contact angle measurement setup. The camera on an iPhone SE was used to take the pictures. An optical lens (50 mm focal length) helped increase the magnification of the images. The center of the drop on the sample stage is set at the focal length. A clamp and stand secured the needle and syringe above the sample stage. (B) Front view of the dynamic contact angle measurement setup. (C) Side view of the dynamic contact angle measurement setup.

surface that is rougher has a higher contact angle compared to the smoother surface.^{9,15,16}

With dynamic contact angle measurement, on the other hand, users determine the transformation of a droplet that is spreading or withdrawing on the surface. From a dynamic contact angle measurement, the hysteresis and kinetics of the interfacial system can be derived.^{15,17–19} So far, there are several methods to measure the dynamics of a liquid on a solid interface from the advancing and receding contact angles. Advancing and receding contact angles can be measured by modifying the volume of the added liquid, tilting the support of the droplet, or introducing air bubbles to the surface of a submerged solid interface.^{14,16,17} The focus of this paper is to develop a simplified needle-in-drop dynamic contact angle measurement assembly for undergraduates to learn about surface properties.

In the needle-in-drop method (Figure 1B), the needle is positioned a few millimeters away from the solid surface, and liquid is gradually dispersed through the needle to create a droplet on the surface.¹⁴ As more liquid is added, the baseline of the droplet in contact with the surface will reach a maximum and then remain constant, causing the droplet to grow only in the vertical direction.¹⁴ Liquid can continually be added to the

droplet until the surface tension can no longer hold the amount of liquid that has been added. At this point, the diameter (baseline) of the droplet against the surface starts to grow again.^{16,17} The maximum contact angle recorded before the surface tension surpasses this limit is the advancing contact angle.¹⁷ Since the drop is changing in size and is not a constant volume, it is called the dynamic measurement.

Many earlier works describing static contact angle measurement apparatus required components to be custom-made with 3D printing^{20,21} or modified from existing systems, such as microscopes^{14,22} In the laboratory training described in this manuscript, students were guided to assemble a simplified needle-in-drop contact angle measurement arrangement as an affordable and effective alternative to commercial goniometers to determine surface properties by performing both static and dynamic contact angle measurements. While static contact angle is frequently used to analyze surfaces,^{1,2,23–26} there are fewer examples, let alone guided laboratory exercises, that describe the usefulness of dynamic contact angle measurements. Dynamic contact angle measurement is important, as the hysteresis calculated from it can be used to further derive kinetic parameters that describe surface homogeneity and energy barriers to liquid spreading at the interface.^{17,27,28}

Employing this approach, crucial information about surface structure, cleanliness, hysteresis, and kinetics of the interfacial properties, relevant in various fields such as materials science, biomedical engineering, and chemistry, can be quickly obtained.

■ HARDWARE ASSEMBLY

The contact angle measurement setup consists of several simple components that are commonly found in an optics lab, as shown in Figure 2. The system was assembled using a screen as the background to create contrast for the droplet outline and the ambient room light. The sample was placed on a sample stage (2" x 3" x 0.3"). Above the sample stage, a 500 μL syringe was positioned to add solvent onto the solid sample surface. The syringe was held in place by a syringe holder, whose design can be customized by the students. A large hole was drilled partially through the top of the holder to allow the syringe to pass, and a smaller hole was drilled from the bottom to allow only the needle of the syringe to pass and hold the rest of the syringe vial in place.

Students can adjust the distance between the syringe needle and the sample surface by changing the height of the sample stage or the height of the syringe from the stand. A ruler was positioned on the sample stage to measure the baseline of the droplet on the sample substrate. In front of the sample stage, a plano-concave lens was fixed at 50 mm, the focal length of the lens. This positioning ensured that the sample stage and the aqueous/sample interface remained at the focal point to have a clear magnified view.

For recording the video of the droplet on the surface, a phone was used in combination with a plano-concave lens. To take pictures or videos, the camera of the phone was focused perpendicularly to the liquid/sample interface,²¹ so that no extra baseline or background was captured. The details of each component in the setup are listed in Table 1.

Table 1. Components Used for Building the Needle-in-Drop Contact Angle Setup

Brand/Maker	Description	Part Number	Quantity
Thorlabs	BK7 A-Coated Plano-Convex Lens, $d=25.4$ mm, $f=50.0$ mm	LA 1131-A	1
Southern Labware	Medium 2-Prong Single Adjust Nickel-Plated Zinc Clamp	0392208	1
Thorlabs	Mounting Base, 1" x 3" x 3/8" (25 x 75 x 10 mm)	BA1	1
Thorlabs	Cap Screw Kit	HW-KIT2/ MM6-1.0 Screws	1
Hamilton	500 μL Syringe	Gastight #1750	1
Thorlabs	1/2" Post Mount	BA2E	1
Thorlabs	1/2" Optical Post, SS, 8-32 Set Screw, 1/4"-20 Tap, L = 4"	TR4	2
Apple	iPhone SE (2nd Edition)	MX9C2LL/A	1
Thorlabs	Background Screen	TPSM2/M	1
Thorlabs	Post Holder with Spring-Loaded Thumb Screw, L = 3"	PH3-ST	1
Thorlabs	Post Holder with Spring-Loaded Thumb Screw, L = 2"	PH2-ST	1
Homemade Design	Sample Stage, 2" x 3" x 0.3"	—	1
Homemade Design	Syringe holder, 2.5 cm x 3.5 cm, Syringe hole diameter = 0.8 cm, Needle hole diameter = 0.5 cm	—	1

■ HAZARDS

The organic solvents used for surface cleaning and contact angle measurements can cause irritation to skin and eyes, inhalation and ingestion can cause damage to organs. The methanol used for surface cleaning is highly flammable. The precursor octadecyltrimethoxysilane (OTMS) (Sigma-Aldrich CAS 3069-42-9) used for coating the fused silica surface can cause severe skin and eye burns upon contact and respiratory irritation if inhaled.

■ CONTACT ANGLE MEASUREMENTS

Contact angle measurements were performed on hydrophobic and hydrophilic substrates. The OTMS coated surface is hydrophobic, which causes the added droplets to form a clear spherical shape on the surface that allows for precise contact angle measurements. A microliter syringe was employed to precisely dispense and withdraw liquid onto the sample surface. Students measured the contact angle of 2 μL of the solvent on a piece of a fused silica wafer (Corning 7980 High Purity Fused Silica, 1.2 cm x 1 cm x 1 mm, cut with a diamond tip) with and without an OTMS coating. These two types of surfaces serve for a comparison, as the fused silica surface is hydrophilic while the OTMS surface is hydrophobic. The procedure for synthesizing a self-assembled monolayer of OTMS on the fused silica surface has been described elsewhere.³⁶ The static contact angle of water on the surface was measured by adding three droplets of DI water with a volume of 2 μL each on three different spots of the surface. The base angles of the droplets on the left and the right were recorded, and the average and standard deviation were calculated to report the accurate static contact angle using these measurements. The contact angle of neutral DI water on OTMS coated fused silica surface is $93.0^\circ \pm 3.8^\circ$ (Table 3, Figure 3). The static contact angle of neutral DI water on the bare silica surface is $18.4^\circ \pm 5.9^\circ$ (Table 3). However, more aggressive cleaning should lead to a smaller contact angle $<10^\circ$.^{10,11} In comparison, the water contact angle on the OTMS coated fused silica surface is more than 70° greater than that on the bare silica surface, indicating a higher degree of hydrophobicity.

The dynamic contact angles were measured by controlling the liquid dispensing and withdrawing rates at 1 $\mu\text{L}/\text{s}$. The measured advancing contact angle of water on the OTMS coated fused silica surface stayed around 96° for 4 s, with a baseline preserved at 3 mm. Subsequently, when the water was withdrawn from the surface, the contact angle reduced to 86° , and the baseline was retained at 1.8 mm for 4 s. Our dynamic contact angle results agree with the findings reported by Koga *et al.*, who observed an advancing contact angle of 92° and a receding contact angle of 88.5° for water on an OTMS monolayer.³⁷ Additionally, our static contact angle result is consistent with the sessile-drop measurement reported by Hild *et al.*, indicating a water contact angle on OTMS is in the range 88.5° – 97.0° .³⁸

Students used the Fiji ImageJ software^{2,23} to measure the contact angle of droplets on the OTMS coated fused silica surface with the "Angle Tool" to draw the tangential line from the droplet/air interface to the solid surface, allowing for precise contact angle measurements. The baseline of the droplet was measured by the scale on the sample stage (Figure 3B).

Table 2. Dynamic and Static Contact Angle Measurement Results of Each Solvent Used to Wet the OTMS Coated Fused Silica Surface

	Surface Tension γ /(mN m ⁻¹)	θ_A /degrees	θ_R /degrees	θ_{static} /degrees
Water (pH 7.2)	72.8 ²⁹	96.2 ± 0.6	85.9 ± 1.4	93.0 ± 3.8
Methanol	22.7 ³⁰	27.9 ± 2.5	21.8 ± 0.1	26.0 ± 4.5
Ethylene Glycol	47.7 ³¹	69.6 ± 2.6	61.4 ± 0.3	70.6 ± 3.5
Glycerol	64.0 ³²	87.9 ± 0.8	73.2 ± 2.7	82.9 ± 2.9
<i>N,N</i> -Dimethylformamide (DMF)	37.1 ³³	48.5 ± 1.2	43.8 ± 0.2	46.6 ± 2.3
Hexane	18.4 ³⁴	11.7 ± 0.4	7.8 ± 0.6	8.7 ± 1.2
Hexadecane	28.5 ^{34,35}	34.8 ± 0.5	23.3 ± 0.2	29.0 ± 4.8
Octadecene	21.6 ²⁴	21.2 ± 1.3	17.8 ± 0.9	19.1 ± 2.8

The mean and standard deviation are calculated from eight individual experiments.

Table 3. Comparison of Static and Dynamic Contact Angles of DI Water on the Fused Silica Surface and the OTMS Coated Fused Silica Surfaces

DI Water	θ_A /degrees	θ_R /degrees	θ_{static} /degrees
OTMS Coated Fused Silica Surface	96.2 ± 0.6	85.9 ± 1.4	93.0 ± 3.8
Fused Silica Surface	22.3 ± 2.5	15.8 ± 3.1	18.4 ± 5.9

The mean and standard deviation are calculated from eight individual experiments.

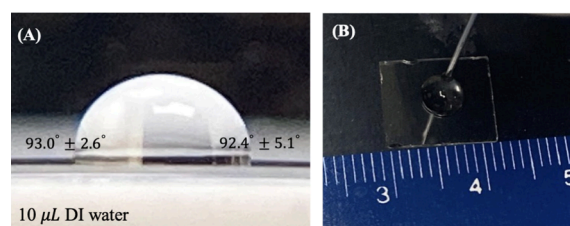


Figure 3. Static contact angle of water on OTMS coated fused silica. (A) Example of a static contact angle measurement using the sessile drop method. The contact angle values reported were calculated from the average of the contact angles measured at the left and the right for multiple droplets. (B) Example image to show how the baseline of the droplet was measured.

To capture the shape transformation of the droplet as the volume of the droplet increased over time, students used the camera on an iPhone SE to record the video at 5–30 frames per second, enabling analysis of the dynamic changes in droplet shape. To ensure precise measurements, the final contact angles were determined by calculating the average of eight individual experiments recorded in distinct videos at corresponding time intervals.

■ CRITICAL SURFACE TENSION OF OTMS ON FUSED SILICA SURFACE

The critical surface tension is a condition in which the surface tension of a liquid equals or overcomes the surface energy of the solid.^{8,9,18} It represents the minimum surface tension required for the liquid to completely wet the entire solid surface.³⁹ Depending on the relative magnitude of the surface energy between the liquid and the solid, the liquid can either form a high contact angle on the solid surface, displaying a low molecular attraction or it can fully spread out the solid surface, presenting a strong molecular attraction.³⁹ In this study, we determined the critical surface tension of an OTMS coated fused silica slide using polar solvents such as water, glycerol, *N,N*-dimethylformamide (DMF), methanol, ethylene glycol, as well as nonpolar solvents including hexane, and hexadecane

(Table 2). The critical surface tension of OTMS-modified fused silica surface was determined using the Fox-Zisman approximation, see eq 2.

$$\cos \theta = 1 - \left(\frac{\gamma - \gamma_c}{\gamma} \right) \quad (2)$$

A rectilinear relationship is established between the cosine of the contact angle, θ , and the surface tension, γ , of a series of solvents.³⁹ The critical surface tension, γ_c , of the OTMS coated fused silica surface is determined by the x -axis intercept of the $\cos \theta$ versus γ plot when $\cos \theta = 1$.³⁹ The relationship between the wettability of nonhomologous solvents on the OTMS coated fused silica surface is shown in Figure 4A, and the value

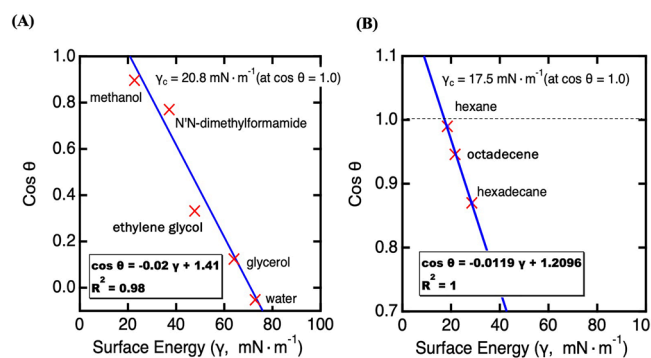


Figure 4. Critical surface tensions of OTMS coated fused silica surface measured by polar solvents and nonpolar solvents. (A) Zisman plot of the critical surface tension of OTMS coated fused silica determined by homologous nonpolar solvents. (B) Zisman plot of the critical surface tension of OTMS coated fused silica determined by nonhomologous polar solvents.

of γ_c is found to be 20.8 mN/m. The relationship between the wettability of homologous solvents on the OTMS coated fused silica surface is shown in Figure 4B, and the value of γ_c is found to be 17.5 mN/m. Homologous solvents with surface energies that closely resemble the critical surface energy of OTMS monolayer, exhibited unhindered spreading on OTMS coated fused silica, resulting in a lower critical surface energy value. Conversely, nonhomologous polar solvents, which are inherently polar and prone to form intermolecular hydrogen bonding, have relatively higher surface free energies, which tends to form higher contact angles on the OTMS monolayer. With a surface critical energy between 17.5 and 20.8 mN/m, the molecular attractions between the OTMS surface and the various solvents investigated here are weak.

CONTACT ANGLE HYSTERESIS AND CONTACT-LINE PINNING FORCE ON OTMS COATED FUSED SILICA

The motion, coalescence, and breakup of a liquid on a surface can be evaluated through contact angle hysteresis measurements, providing valuable information on liquid dynamics on surfaces for fields such as microfluidics, inkjet printing, and surface coating. The contact angle hysteresis is the frictional energy that impedes the movement of the liquid on the surface. It is important as it indicates the amount of kinetic energy required for the liquid to transition from its metastable state to a dynamic state.²⁷ Here, the advancing and receding contact angles of water on the OTMS coated fused silica surface reduced over time along with the corresponding baseline as presented in Figure 5. The contact angle hysteresis, $\Delta\theta$, is

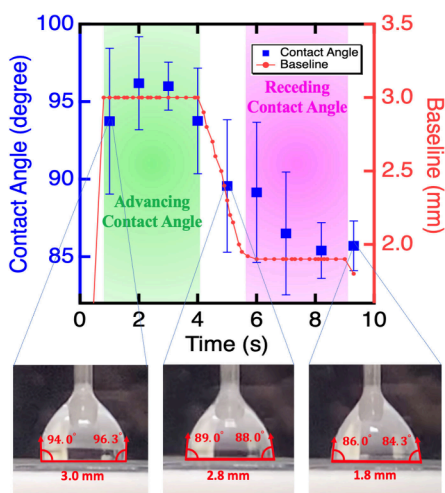


Figure 5. Advancing and receding contact angles and the baseline of a water droplet were measured at a flow rate of 1 μL per second, added every second, at $T = 18.4\text{ }^\circ\text{C}$ and $\text{RH} = 21\%$. Images at the bottom are of the liquid drop in contact with the OTMS coated fused silica surface at different times as the volume of liquid added increases. Data is based on approximately 8 frames per second video.

calculated using eq 3.²⁷ By incorporating the measured advancing and receding contact angles of water on the OTMS coated fused silica surface, the contact angle hysteresis was determined to be $10^\circ \pm 2^\circ$.

$$\Delta\theta = \theta_A - \theta_R \quad (3)$$

The obtained values of the contact angle hysteresis and the base radius of the droplet were employed to derive the contact-line pinning force, as described in eq 4.⁴⁰

$$F_{\text{pinning}} = 2\gamma r(\cos \theta_R - \cos \theta_A) \quad (4)$$

The contact-line pinning force, denoted as F_{pinning} , is associated with the resistance encountered during the spreading and withdrawing of a liquid on a solid surface.⁴⁰ This force depends on the liquid surface tension, γ , the base radius, r , and the difference of the cosine of receding contact angle and advancing contact angle. The pinning force acts as a barrier, impeding the movement of the contact-line. For water moving on the OTMS coated fused silica surface in response to time, the resultant contact-line pinning force is shown in Figure 6.

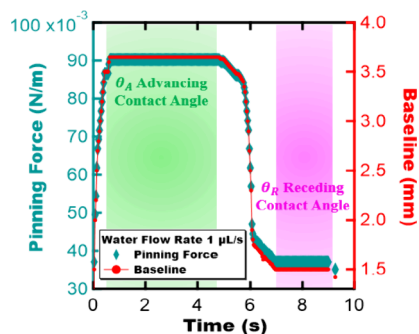


Figure 6. Contact-line pinning force of water on the OTMS coated fused silica surface changes in correspondence with the baseline recorded along the time scale of the advancing contact angle and the receding contact angle. Data is based on approximately 30 frames per second video.

LEARNING OUTCOMES AND ASSESSMENT

This static and dynamic contact angle experiment aims to equip undergraduates with the skills and understanding necessary for liquid/solid interface characterization. Through this hands-on experience (Figure 7), students will gain insights into the fundamental principles of surface chemistry and learn how chemical modifications at the molecular level can significantly influence macroscopic surface properties. This training is expected to provide students practical knowledge that is applicable across wide-ranging disciplines in fields such as material science, nanotechnology, biomedical engineering, and surface coatings.

The primary goal of this training was to enhance students' understanding of static and dynamic contact angle measurements and related concepts such as surface tension, surface free energy, hydrophobicity, hydrophilicity, the dynamic contact angle, contact angle hysteresis, and contact line pinning force, etc.

As a prelab preparation, students were provided with reading materials covering key concepts. On average, each student spent approximately 30 min reading the materials. Then, before the experiment, the prelab quiz was conducted to assess the student's understanding of the provided materials. After the prelab quiz (supplied in the Supporting Information), students engaged in the hands-on experiment involving the preparation of an OTMS monolayer on the fused silica glass, followed by performing contact angle measurements in pairs and data analysis using ImageJ.

In the prelab quiz, out of 8 students, 7 students scored 9/10, 1 student scored 8/10, and 1 student scored 10/10. The scores suggest a strong baseline understanding of the basic concepts among most participants after only spending a short time reviewing the materials. To provide students a chance to apply these concepts to practical scenarios, hands-on training was provided. This focused on building upon the students' existing knowledge base and expanding their understanding of both theoretical and practical aspects of surface chemistry.

After the contact angle measurement, students were asked to analyze the data using ImageJ and calculate the advancing and receding contact angles for both bare and OTMS-coated fused silica. From the dynamic contact angle data, students were able to calculate the contact angle hysteresis. Students' dynamic contact angle data is in accordance with the reported value for OTMS-coated fused silica, suggesting that the students were able to successfully deposit OTMS on fused silica and obtain

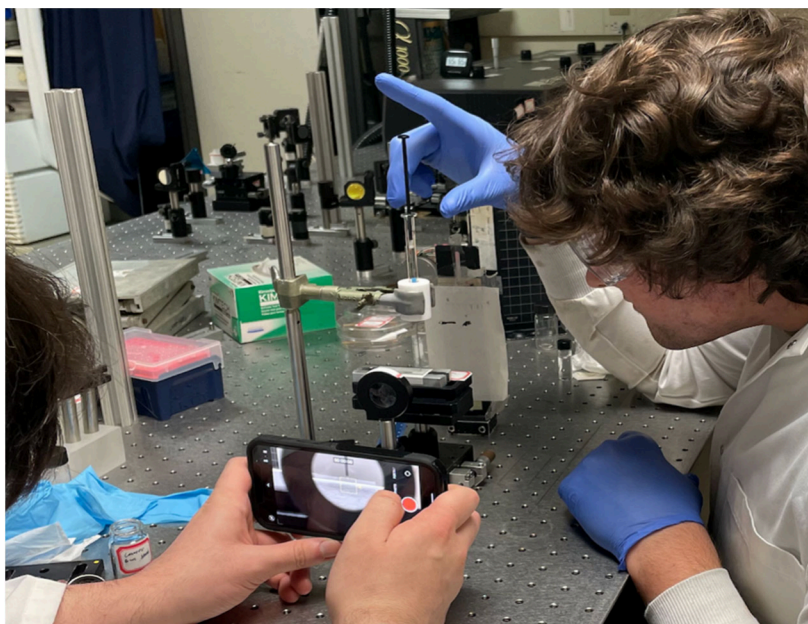


Figure 7. Students are doing contact angle measurements using the setup assembled with common lab components and recording the droplet behavior on the surface using their phone.

Table 4. Undergraduate Training Learning Objectives, Laboratory Activities, and Assessment Checkpoints

Learning objective	Activity	Checkpoint
Develop an understanding of surface properties realed by contact angle measurements	Before the lab, students read the given resources of the following topics: surface tension, surface wettability, contact angle (static vs dynamic), contact-line pinning force. After the reading, students took the prelab quiz to evaluate their fundamental understanding.	Prelab quiz
Introduce students to the equipment assembly, substrate preparation and cleaning	Demonstrated and trained students how to prepare OTMS coated substrate, and how to clean substrates and syringes before the experiment.	Graduate students check if there are residue from the reflection of substrates
Static and dynamic contact angle measurements	Use needle-in-drop method to perform static, advancing, and receding contact angle measurements. Record the contact angles by camera.	Contact angles recorded in photos and videos
Contact angle data extraction, plotting and analysis	Guide students using ImageJ software to analyze contact angles, present the results into a plot, and calculate hysteresis, contact-line pinning force	Results plot and postlab test

its characterization through contact angle measurements using the setup described here.

To evaluate the development of student comprehension and problem solving skills following the training session, students were tested by postlab questions (provided in the [Supporting Information](#)) requiring free-response answers. The students' answers to the postlab questions were assessed following a standard grading rubric that was discussed and created by the authors. The students' answers revealed that they encountered difficulties understanding formulas like Young's Equation and Pinning Force calculations. Out of the eight trained students, only four could provide a comprehensive explanation of each parameter and what it means to achieve equilibrium in the Young's Equation. Only one student could accurately calculate the pinning-force, with others struggling on the unit of surface tension. Despite this, students exhibit strong comprehension and memorization of theoretical concepts and pictorial illustrations. Most could clearly define hydrophilic and hydrophobic and estimate the corresponding contact angles ranges. To address the weakness in the students' understanding, we suggest that instructors demonstrate the calculations of Young's Equation and Pinning Force to students. This will provide students a good review of the variables and their units. Additionally, inductive training, such as drawing the chemical structures and the possible binding

motifs of the liquid molecules to the surface functional groups, may encourage deeper scientific thinking among students.

Overall, after this contact angle experimental training, students have developed the following skills and understandings (Table 4):

- Utilization of simple components to assemble a user-friendly setup for static and dynamic contact angle measurements.
- Proper cleaning of the measurement syringe (plunger, barrel, hub, and needle) and sample surfaces using sonication, organic solvent, and nitrogen gas purging.
- Record the contact angle precisely using the camera on the phone.
- Master the ImageJ software for analyzing contact angles and baselines from droplet images on the substrate surface.
- Determine whether the surface is hydrophilic or hydrophobic from the magnitude of the contact angle.
- Provide statistical analysis for multiple data and present the results in trend plots.
- Calculate the hysteresis and the contact-line pinning force of the measured substrate.

In the end, students were invited to share their feedback on the training. From their responses, it was revealed that for all of them, it was their first hands-on experiment focused on

interfacial phenomena. This concept is important in chemistry and other related fields because the interface is often where reactions are initiated and occur. The feedback of students underscores the importance of involving comprehensive explanations and experimental explorations of interfaces into chemistry curriculums. Emphasizing these aspects in future courses will provide students with an understanding of how contact angle measurements describe liquid-surface interactions and can disclose chemical reactions at interfaces.^{26,41,42}

CONCLUSIONS

In conclusion, we have developed an easy-to-assemble dynamic contact angle measurement setup, enabling us to capture the dynamic transformations occurring at the liquid–solid interface. The accuracy and stability of our dynamic contact angle measurements were demonstrated by comparing our results with the results from previous publications. This encompassed a broad range of quantifiable angles, including those above 90° and below 25°. By analyzing the advancing and receding contact angles and the baseline of the liquid on the solid surface, we were able to determine crucial parameters such as contact angle hysteresis and contact-line pinning force. The application of this setup extends beyond a research environment, as it can be effectively employed in chemistry laboratory classes to illustrate the physical and chemical interactions taking place at the solid–liquid interface. Furthermore, it holds significant potential for surface measurements in diverse research fields, including materials science and surface coating.

ASSOCIATED CONTENT

Supporting Information

The Supporting Information is available at <https://pubs.acs.org/doi/10.1021/acs.jchemed.4c00146>.

Contact angle measurements training lab manual, contact angle measurements prelab questions, contact angle measurements prelab questions grading rubric, contact angle measurements postlab questions, contact angle measurements postlab questions grading rubric, contact angle training results for reference (PDF)

AUTHOR INFORMATION

Corresponding Author

Eric Borguet – Department of Chemistry, Temple University, Philadelphia, Pennsylvania 19122, United States;
orcid.org/0000-0003-0593-952X; Email: eborguet@temple.edu

Authors

Yunqian Zou – Department of Chemistry, Temple University, Philadelphia, Pennsylvania 19122, United States;
orcid.org/0000-0003-3355-3528
Naomi Ross – Department of Chemistry, Temple University, Philadelphia, Pennsylvania 19122, United States;
orcid.org/0000-0003-4657-0327
Wasim Nawaj – Department of Chemistry, Temple University, Philadelphia, Pennsylvania 19122, United States

Complete contact information is available at:
<https://pubs.acs.org/10.1021/acs.jchemed.4c00146>

Notes

The authors declare no competing financial interest.

ACKNOWLEDGMENTS

The authors thank Robert Castillo, Liam Gannon, Lauren Towers, Jessica Kolora, Samy Mohan, Souvik Pramanick, and Belinta Simiyu from the Borguet Lab for participating in contact angle measurement training, and Matthew McCormick from the College of Science and Technology of Temple University machine shop for making the syringe holder and sample stage. E.B. acknowledges the support of the National Science Foundation under grant CHE 2102557.

REFERENCES

- (1) Ihrig, J. L.; Lai, D. Y. F. Contact angle measurement. *J. Chem. Educ.* **1957**, *34* (4), 196.
- (2) Lamour, G.; Hamraoui, A.; Buvailo, A.; Xing, Y.; Keuleyan, S.; Prakash, V.; Eftekhari-Bafrooei, A.; Borguet, E. Contact Angle Measurements Using a Simplified Experimental Setup. *J. Chem. Educ.* **2010**, *87* (12), 1403–1407.
- (3) Rotenberg, Y.; Boruvka, L.; Neumann, A. W. Determination of surface tension and contact angle from the shapes of axisymmetric fluid interfaces. *J. Colloid Interface Sci.* **1983**, *93* (1), 169–183.
- (4) Cai, H.; Fan, H.; Zhao, L.; Hong, H.; Shen, L.; He, Y.; Lin, H.; Chen, J. Effects of surface charge on interfacial interactions related to membrane fouling in a submerged membrane bioreactor based on thermodynamic analysis. *J. Colloid Interface Sci.* **2016**, *465*, 33–41.
- (5) Kato, A. N.; Jiang, Y.; Chen, W.; Seto, R.; Li, T. How surface roughness affects the interparticle interactions at a liquid interface. *J. Colloid Interface Sci.* **2023**, *641*, 492–498.
- (6) Buckley, J. S.; Takamura, K.; Morrow, N. R. Influence of Electrical Surface Charges on the Wetting Properties of Crude Oils. *SPE Reservoir Engineering* **1989**, *4* (03), 332–340.
- (7) Law, K.-Y. Definitions for Hydrophilicity, Hydrophobicity, and Superhydrophobicity: Getting the Basics Right. *J. Phys. Chem. Lett.* **2014**, *5* (4), 686–688.
- (8) Schrader, M. E. Young-Dupre Revisited. *Langmuir* **1995**, *11* (9), 3585–3589.
- (9) Lamour, G.; Eftekhari-Bafrooei, A.; Borguet, E.; Souès, S.; Hamraoui, A. Neuronal adhesion and differentiation driven by nanoscale surface free-energy gradients. *Biomaterials* **2010**, *31* (14), 3762–3771.
- (10) Wang, R.; Zou, Y.; Remsing, R. C.; Ross, N. O.; Klein, M. L.; Carnevale, V.; Borguet, E. Superhydrophilicity of α -alumina surfaces results from tight binding of interfacial waters to specific aluminols. *J. Colloid Interface Sci.* **2022**, *628*, 943–954.
- (11) Zhang, D.; Wang, Y.; Gan, Y. Characterization of critically cleaned sapphire single-crystal substrates by atomic force microscopy, XPS and contact angle measurements. *Appl. Surf. Sci.* **2013**, *274*, 405–417.
- (12) Svoboda, M.; Malijevský, A.; Lísal, M. Wetting properties of molecularly rough surfaces. *J. Chem. Phys.* **2015**, *143* (10), 104701.
- (13) Birch, W.; Carré, A.; Mittal, K. L. 13 - Wettability Techniques to Monitor the Cleanliness of Surfaces. In *Developments in Surface Contamination and Cleaning*, Kohli, R., Mittal, K. L., Eds.; William Andrew Publishing, 2008; pp 693–723.
- (14) Albert, E.; Tegze, B.; Hajnal, Z.; Zámbo, D.; Szekrényes, D. P.; Deák, A.; Hörvölgyi, Z.; Nagy, N. Robust Contact Angle Determination for Needle-in-Drop Type Measurements. *ACS Omega* **2019**, *4* (19), 18465–18471.
- (15) Law, K.-Y. Contact Angle Hysteresis on Smooth/Flat and Rough Surfaces. Interpretation, Mechanism, and Origin. *Accounts of Mater. Res.* **2022**, *3* (1), 1–7.
- (16) Lei, D.; Li, Y.; Lin, M.; Wen, M. Model of Advancing and Receding Contact Angles on Rough Surfaces. *J. Phys. Chem. C* **2019**, *123* (30), 18376–18386.
- (17) Bracke, M.; De Voeght, F.; Joos, P. *The Kinetics of Wetting: The Dynamic Contact Angle*, Vol. 79; 2007; pp 142–149.
- (18) Zisman, W. A. Relation of the Equilibrium Contact Angle to Liquid and Solid Constitution. In *Contact Angle, Wettability, and*

Adhesion, Advances in Chemistry, Vol. 43; American Chemical Society, 1964; pp 1–51.

(19) Davidson, R. D.; O'Loughlin, T. E.; Alivio, T. E. G.; Lim, S.-M.; Banerjee, S. Thermodynamics of Wettability: A Physical Chemistry Laboratory Experiment. *J. Chem. Educ.* **2022**, *99* (7), 2689–2696.

(20) Crowe, C. D.; Hendrickson-Stives, A. K.; Kuhn, S. L.; Jackson, J. B.; Keating, C. D. Designing and 3D Printing an Improved Method of Measuring Contact Angle in the Middle School Classroom. *J. Chem. Educ.* **2021**, *98* (6), 1997–2004.

(21) Han, W.; Shin, J.; Ho Shin, J. Low-cost, open-source contact angle analyzer using a mobile phone, commercial tripods and 3D printed parts. *HardwareX* **2022**, *12*, No. e00327.

(22) Dionísio, M.; Sotomayor, J. A Surface Chemistry Experiment Using an Inexpensive Contact Angle Goniometer. *J. Chem. Educ.* **2000**, *77* (1), 59.

(23) Khan, M. S.; Wani, A. A.; Jan, Q.; Bhat, M. M.; Kuchey, M. Y.; Sheikh, U. R.; Sofi, F. A.; Bhat, M. A. Smartphone-Assisted Contact Angle Measurements: A Simple Approach to Determine the Critical Micelle Concentration of Surfactants. *J. Chem. Educ.* **2024**, *101* (3), 1198–1203.

(24) Coffinier, Y.; Piret, G.; Das, M. R.; Boukherroub, R. Effect of surface roughness and chemical composition on the wetting properties of silicon-based substrates. *Comptes Rendus Chimie* **2013**, *16*, 65–72.

(25) Massoumi, H.; Chug, M. K.; Nguyen, G. H.; Brisbois, E. J. A Multidisciplinary Experiment to Characterize Antifouling Biocompatible Interfaces via Quantification of Surface Protein Adsorption. *J. Chem. Educ.* **2022**, *99* (7), 2667–2676.

(26) Ye, T.; Wynn, D.; Dudek, R.; Borguet, E. Photoreactivity of Alkylsiloxane Self-Assembled Monolayers on Silicon Oxide Surfaces. *Langmuir* **2001**, *17* (15), 4497–4500.

(27) Eral, H. B.; 't Mannetje, D. J. C. M.; Oh, J. M. Contact angle hysteresis: a review of fundamentals and applications. *Colloid Polym. Sci.* **2013**, *291* (2), 247–260.

(28) Li, X.; Bodziony, F.; Yin, M.; Marschall, H.; Berger, R.; Butt, H. J. Kinetic drop friction. *Nat. Commun.* **2023**, *14* (1), 4571.

(29) Vargaftik, N. B.; Volkov, B. N.; Voljak, L. D. International Tables of the Surface Tension of Water. *J. Phys. Chem. Ref. Data* **1983**, *12* (3), 817–820.

(30) Niraula, T. P.; Shah, S. K.; Chatterjee, S. K.; Bhattarai, A. Effect of methanol on the surface tension and viscosity of sodiumdodecyl sulfate (SDS) in aqueous medium at 298.15–323.15 K. *Karbala International Journal of Modern Science* **2018**, *4* (1), 26–34.

(31) Velasco-Medina, A. A.; Gracia-Fadrique, J. Surface Tension and Density of Ethylene Glycol Monobutyl Ether–Water Mixtures from 277.15 to 308.15 K. *Journal of Chemical & Engineering Data* **2020**, *65* (9), 4547–4555.

(32) Takamura, K.; Fischer, H.; Morrow, N. R. Physical properties of aqueous glycerol solutions. *J. Pet. Sci. Eng.* **2012**, *98–99*, 50–60.

(33) Rafati, A. A.; Ghasemian, E.; Iloukhani, H. Surface Tension and Surface Properties of Binary Mixtures of 1,4-Dioxane or N,N-Dimethyl Formamide with n-Alkyl Acetates. *Journal of Chemical & Engineering Data* **2009**, *54* (12), 3224–3228.

(34) Klein, T.; Yan, S.; Cui, J.; Magee, J. W.; Kroenlein, K.; Rausch, M. H.; Koller, T. M.; Fröba, A. P. Liquid Viscosity and Surface Tension of n-Hexane, n-Octane, n-Decane, and n-Hexadecane up to 573 K by Surface Light Scattering. *Journal of Chemical & Engineering Data* **2019**, *64* (9), 4116–4131.

(35) Rolo, L. I.; Caço, A. I.; Queimada, A. J.; Marrucho, I. M.; Coutinho, J. A. P. Surface Tension of Heptane, Decane, Hexadecane, Eicosane, and Some of Their Binary Mixtures. *Journal of Chemical & Engineering Data* **2002**, *47* (6), 1442–1445.

(36) Nihonyanagi, S.; Eftekhari-Bafrooei, A.; Hines, J.; Borguet, E. Self-Assembled Monolayer Compatible with Metal Surface Acoustic Wave Devices on Lithium Niobate. *Langmuir* **2008**, *24* (9), 5161–5165.

(37) Koga, T.; Morita, M.; Ishida, H.; Yakabe, H.; Sasaki, S.; Sakata, O.; Otsuka, H.; Takahara, A. Dependence of the Molecular

Aggregation State of Octadecylsiloxane Monolayers on Preparation Methods. *Langmuir* **2005**, *21* (3), 905–910.

(38) Hild, R.; David, C.; Müller, H. U.; Völkel, B.; Kayser, D. R.; Grunze, M. Formation and Characterization of Self-assembled Monolayers of Octadecyltrimethoxysilane on Chromium: Application in Low-Energy Electron Lithography. *Langmuir* **1998**, *14* (2), 342–346.

(39) Shafrin, E. G.; Zisman, W. A. Critical surface tension for spreading on a liquid substrate. *J. Phys. Chem.* **1967**, *71* (5), 1309–1316.

(40) Barrio-Zhang, H.; Ruiz-Gutiérrez, É.; Armstrong, S.; McHale, G.; Wells, G. G.; Ledesma-Aguilar, R. Contact-Angle Hysteresis and Contact-Line Friction on Slippery Liquid-like Surfaces. *Langmuir* **2020**, *36* (49), 15094–15101.

(41) McArthur, E. A.; Ye, T.; Cross, J. P.; Petoud, S.; Borguet, E. Fluorescence Detection of Surface-Bound Intermediates Produced from UV Photoreactivity of Alkylsiloxane SAMs. *J. Am. Chem. Soc.* **2004**, *126* (8), 2260–2261.

(42) Ye, T.; McArthur, E. A.; Borguet, E. Mechanism of UV Photoreactivity of Alkylsiloxane Self-Assembled Monolayers. *J. Phys. Chem. B* **2005**, *109* (20), 9927–9938.